Null-Field Integral Equation Approach for Plate Problems With Circular Boundaries

Jeng-Tzong Chen
e-mail: jtchen@mail.ntou.edu.tw

Chia-Chun Hsiao

Department of Harbor and River Engineering,
National Taiwan Ocean University,
No. 2, Pei-Ning Road,
Keelung 20224, Taiwan

Shyue-Yuh Leu
Hydraulic Engineering Department,
Sinotech Engineering Consultants,
171 Nanking E. Road, Sec. 5,
Taipei 10570, Taiwan

In this paper, a semi-analytical approach for circular plate problems with multiple circular holes is presented. Null-field integral equation is employed to solve the plate problems while the kernel functions in the null-field integral equation are expanded to degenerate kernels based on the separation of field and source points in the fundamental solution. The unknown boundary densities of the circular plates are expressed in terms of Fourier series. It is noted that all the improper integrals are transformed to series sum and are easily calculated when the degenerate kernels and Fourier series are used. By matching the boundary conditions at the collocation points, a linear algebraic system is obtained. After determining the unknown Fourier coefficients, the displacement, slope, normal moment, and effective shear force of the plate can be obtained by using the boundary integral equations. Finally, two numerical examples are proposed to demonstrate the validity of the present method and the results are compared with the available exact solution, the finite element solution using ABAQUS software and the data of Bird and Steele. [DOI: 10.1115/1.2165239]

1 Introduction

The boundary element method (BEM) by discretizing the boundary integral equation (BIE) has been extensively applied to engineering problems recently more than domain type methods, e.g., finite element method (FEM) or finite difference method. It is noted that improper integrals on the boundary should be handled particularly when BEM is used. In the past, many researchers proposed several regularization techniques to deal with the singularity and hypersingularity. To determine the Cauchy principal value and the Hadamard principal value in the singular and hypersingular integrals is a critical issue in BEM/BIEM [1]. The technique of the integration by parts to reduce the order of singularity [2] is an alternative. One order of singularity is shifted to the density function from the kernel. In this paper, instead of using the previous concepts, the kernel function is described in an analytical form on each side (interior and exterior) by employing the separable kernel since the potential is discontinuous across the boundary. Therefore, degenerate kernel, namely separable kernel, is a vital tool to study the perforated plate which satisfies the biharmonic equation.

BIEs for the plate problems were acquired from the Rayleigh-Green identity [3,4] and the null-field integral equations were derived by collocating the field point outside the domain. Null-field integral equation in conjunction with degenerate kernel is proposed to solve the biharmonic problems with circular boundaries. It is well known that Fourier series is always incorporated to formulate the solution for problems with circular boundaries [5–8]. Bird and Steele [5] presented a Fourier series procedure to solve circular plate problems containing multiple circular holes in a similar way to the Trefftz method by adopting the interior and exterior T-complete sets. Either the interior or exterior bases in the Trefftz method are embedded in degenerate kernels [9]. A bridge to connect the Trefftz method and method of fundamental solution was constructed by using the degenerate kernels [9]. The Fourier series procedure can solve the circular plate problems regardless of the number, location, and size of circular holes. Also, Crouch and Mogilevskaya [6] presented a method for solving problems with circular boundaries. Their formulation is based on real-variable approach. Mogilevskaya and Crouch [8] have used the Galerkin method instead of collocation technique. Our approach can be extended to the Galerkin formulation only for the circular and annular cases. However, it may encounter difficulty for the eccentric example. Two requirements are needed: degenerate kernel expansion must be available and distinction of interior and exterior expression must be separated. Therefore, the collocation angle of f is not in the range 0 to $2p$ in our adaptive observer system. This is the reason why we cannot formulate in terms of Galerkin formulation using orthogonal properties twice. Free of worrying how to choose the collocation points, uniform collocation along the circular boundary yields a well-posed matrix. On the other hand, Bird and Steele [5] have also used separated solution procedure for bending of circular plates with circular holes in a similar way to the Trefftz method and addition theorem. They used the so-called method of series and addition theorem. Addition theorems are re-expansion formulas for the special functions (e.g., Bessel function, Legendre functions, surface spherical harmonics, etc.) in a transferred coordinate system (see, e.g., Gradshteyn and Ryzhik Table of Integrals [7]). Bird and Steele sought the solution of the original problem as the superposition of the solutions for a single hole problem. After taking the limit to the boundary of each hole, Bird and Steele got the equation that linked the Fourier series with the known coefficients used to approximate the boundary condition with the Fourier series with the unknown coefficients obtained from the solution process. The Fourier series from both sides of the equation were written in the same coordinate system, so the unknown coefficients were found by using orthogonal properties of the terms involved in the Fourier series [10]. To the authors' best knowledge, null-field integral equations and degenerate kernels were not employed to fully capture the circular boundaries although Fourier series expansion was used in previous research [5,6,8,11]. Jeffery [12] and Ling [13] adopted the bipolar coordinate system to derive the solution of stress for the plate problems since it is recognized as the best treatment for analyzing the biharmonic problem with two circular boundaries. Nevertheless, an analytical approach may be hindered

Contributed by the Applied Mechanics Division of ASME for publication in the JOURNAL OF APPLIED MECHANICS. Manuscript received August 5, 2005; final manuscript received October 18, 2005. Review conducted by S. Mukherjee. Discussion on the paper should be addressed to the Editor, Prof. Robert M. McMeeking, JOURNAL OF APPLIED MECHANICS, Department of Mechanical and Environmental Engineering, University of California – Santa Barbara, Santa Barbara, CA 93106-5070, and will be accepted until four months after final publication in the paper itself in the ASME JOURNAL OF APPLIED MECHANICS.

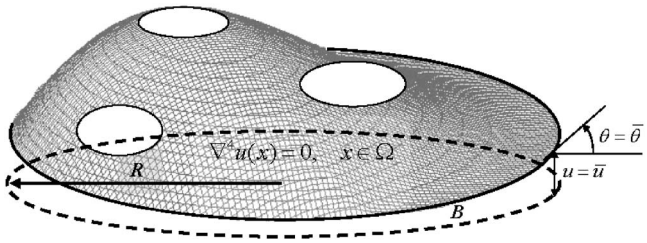

Fig. 1 The perforated Kirchhoff plate subject to the essential boundary conditions

for the complicated problems with more than two holes. Developing a systematic method to solve problems with several holes is not trivial.

The purpose of this paper is to study biharmonic problems with circular boundaries by using the null-field integral formulation in conjunction with degenerate kernels and Fourier series. According to the degenerate kernels, null-field integral formulation and Fourier series in the adaptive coordinate system, a linear algebraic system is constructed by matching the boundary conditions at the collocation points. After determining the Fourier coefficients, the displacement, slope, moment, and shear force of the plate with circular boundaries can be obtained by using the boundary integral equations for the domain point. In the polar coordinate system, the calculation of potential gradients in the normal and tangential directions for the non-concentric domain must be determined with care. Therefore, the technique of vector decomposition is adopted to deal with the problem for the non-concentric plate. Finally, several examples are presented to show the validity of the present method and some conclusions are made.

2 Problems Statement for a Plate

Consider a Kirchhoff plate for the two-dimensional domain under the distributed load $w(x)$, the governing equation is written as follows

$$\nabla^4 u^*(x) = \frac{w(x)}{D}, \quad x \in \Omega \tag{1}$$

where $u^*(x)$ is the lateral displacement, Ω is the domain of the thin plate, D is the flexural rigidity of the plate which is expressed as

$$D = \frac{Eh^3}{12(1-\nu^2)} \tag{2}$$

in which E is Young's modulus, ν denotes the Poisson ratio, and h is the plate thickness. For simplicity, the clamped case is considered

$$u^*(x) = 0, \quad \theta^*(x) = 0, \quad x \in B \tag{3}$$

where B is the boundary of the domain and $\theta^*(x)$ is the slope. Since the governing equation contains the body force, Eq. (1) can be reformulated to the homogeneous equation by using the splitting method as follows

$$\nabla^4 u(x) = 0, \quad x \in \Omega \tag{4}$$

and the essential boundary conditions are changed to

$$u(x) = \bar{u}(x), \quad \theta(x) = \bar{\theta}(x), \quad x \in B \tag{5}$$

as shown in Fig. 1, where $u(x)$ is the displacement and $\theta(x)$ is the slope of the plate.

3 Formulation

3.1 Integral Equation for the Collocation Point in the Domain. The boundary integral equations for the domain point can be derived from the Rayleigh-Green identity [3,4] as follows

$$8\pi u(x) = -\int_B U(s,x)v(s)dB(s) + \int_B \Theta(s,x)m(s)dB(s) - \int_B M(s,x)\theta(s)dB(s) + \int_B V(s,x)u(s)dB(s), \quad x \in \Omega \tag{6}$$

$$8\pi \theta(x) = -\int_B U_\theta(s,x)v(s)dB(s) + \int_B \Theta_\theta(s,x)m(s)dB(s) - \int_B M_\theta(s,x)\theta(s)dB(s) + \int_B V_\theta(s,x)u(s)dB(s), \quad x \in \Omega \tag{7}$$

$$8\pi m(x) = -\int_B U_m(s,x)v(s)dB(s) + \int_B \Theta_m(s,x)m(s)dB(s) - \int_B M_m(s,x)\theta(s)dB(s) + \int_B V_m(s,x)u(s)dB(s), \quad x \in \Omega \tag{8}$$

$$8\pi v(x) = -\int_B U_v(s,x)v(s)dB(s) + \int_B \Theta_v(s,x)m(s)dB(s) - \int_B M_v(s,x)\theta(s)dB(s) + \int_B V_v(s,x)u(s)dB(s), \quad x \in \Omega \tag{9}$$

where B is the boundary of the domain Ω, $u(x)$, $\theta(x)$, $m(x)$, and $v(x)$ are the displacement, slope, moment, and shear force, s and x mean the source and field points, respectively. The kernel functions U, Θ, M, V, U_θ, Θ_θ, M_θ, V_θ, U_m, Θ_m, M_m, V_m, U_v, Θ_v, M_v, V_v in Eqs. (6)–(9), which are expanded to degenerate kernels by using the separation of source and field points, will be elaborated on later. The kernel function $U(s,x)$ in Eq. (6) is the fundamental solution which satisfies

$$\nabla^4 U(s,x) = 8\pi\delta(s-x) \tag{10}$$

where $\delta(s-x)$ is the Dirac-delta function. Therefore, the fundamental solution can be obtained

$$U(s,x) = r^2 \ln r \tag{11}$$

where r is the distance between the source point s and field point x. The relationship among $u(x)$, $\theta(x)$, $m(x)$, and $v(x)$ is shown as follows

$$\theta(x) = K_{\theta,x}(u(x)) = \frac{\partial u(x)}{\partial n_x} \tag{12}$$

$$m(x) = K_{m,x}(u(x)) = \nu\nabla_x^2 u(x) + (1-\nu)\frac{\partial^2 u(x)}{\partial^2 n_x} \tag{13}$$

$$v(x) = K_{v,x}(u(x)) = \frac{\partial \nabla_x^2 u(x)}{\partial n_x} + (1-\nu)\frac{\partial}{\partial t_x}[n_i(x)t_j(x)u_{,ij}(x)] \tag{14}$$

where $K_{\theta,x}(\cdot)$, $K_{m,x}(\cdot)$, $K_{v,x}(\cdot)$ are the slope, moment, and shear force operators with respect to the point x, $\partial/\partial n_x$ is the normal derivative with respect to the field point x, $\partial/\partial t_x$ is the tangential derivative with respect to the field point x, ∇_x^2 means the Laplacian operator, and ν is the Poisson ratio.

3.2 Null-Field Integral Equations. The null-field integral equations are obtained by collocating the field point x outside the domain as follows

$$0 = -\int_B U(s,x)v(s)dB(s) + \int_B \Theta(s,x)m(s)dB(s) - \int_B M(s,x)\theta(s)dB(s) + \int_B V(s,x)u(s)dB(s), \quad x \in \Omega^C \tag{15}$$

$$0 = -\int_B U_\theta(s,x)v(s)dB(s) + \int_B \Theta_\theta(s,x)m(s)dB(s) - \int_B M_\theta(s,x)\theta(s)dB(s) + \int_B V_\theta(s,x)u(s)dB(s), \quad x \in \Omega^C \tag{16}$$

$$0 = -\int_B U_m(s,x)v(s)dB(s) + \int_B \Theta_m(s,x)m(s)dB(s) - \int_B M_m(s,x)\theta(s)dB(s) + \int_B V_m(s,x)u(s)dB(s), \quad x \in \Omega^C \tag{17}$$

$$0 = -\int_B U_v(s,x)v(s)dB(s) + \int_B \Theta_v(s,x)m(s)dB(s) - \int_B M_v(s,x)\theta(s)dB(s) + \int_B V_v(s,x)u(s)dB(s), \quad x \in \Omega^C \tag{18}$$

where Ω^C is the complementary domain of Ω. Since the four equations of Eqs. (15)–(18) in the plate formulation are provided, there are six (C_2^4) options for choosing any two equations to solve the problems. For simplicity, Eqs. (15) and (16) are used to analyze the plate problems. In the real implementation, the point in the null-field integral equation is moved to the boundary from Ω^C such that the kernel functions can be expressed in terms of appropriate forms of degenerate kernels. Novelly, all the improper integrals disappear and transform to series sum in the BIEs since the potential across the boundary can be determined in both sides by using degenerate kernels.

3.3 Expansion of Fourier Series for Boundary Densities. The displacement $u(s)$, slope $\theta(s)$, moment $m(s)$, and shear force $v(s)$ along the circular boundaries in the null-field integral equations are expanded in terms of Fourier series, which are expressed as follows

$$u(s) = c_0 + \sum_{n=1}^{M} (c_n \cos n\theta + d_n \sin n\theta), \quad s \in B \tag{19}$$

$$\theta(s) = g_0 + \sum_{n=1}^{M} (g_n \cos n\theta + h_n \sin n\theta), \quad s \in B \tag{20}$$

$$m(s) = a_0 + \sum_{n=1}^{M} (a_n \cos n\theta + b_n \sin n\theta), \quad s \in B \tag{21}$$

$$v(s) = p_0 + \sum_{n=1}^{M} (p_n \cos n\theta + q_n \sin n\theta), \quad s \in B \tag{22}$$

where a_0, a_n, b_n, c_0, c_n, d_n, g_0, g_n, h_n, p_0, p_n, and q_n are the Fourier coefficients and M is the number of Fourier series terms.

3.4 Expansion of Kernels. By employing the separation technique for the source and field points, the kernel function $U(s,x)$ can be expanded in terms of degenerate kernel in a series form [14] as shown in the following

$$U(s,x) = r^2 \ln r = \begin{cases} U^I(s,x) = \rho^2(1+\ln R) + R^2 \ln R - \left[R\rho(1+2\ln R) + \frac{1}{2}\frac{\rho^3}{R}\right]\cos(\theta-\phi) \\ \quad -\sum_{m=2}^{\infty}\left[\frac{1}{m(m+1)}\frac{\rho^{m+2}}{R^m} - \frac{1}{m(m-1)}\frac{\rho^m}{R^{m-2}}\right]\cos[m(\theta-\phi)], \quad R \geqslant \rho \qquad (23a) \\ U^E(s,x) = R^2(1+\ln \rho) + \rho^2 \ln \rho - \left[\rho R(1+2\ln \rho) + \frac{1}{2}\frac{R^3}{\rho}\right]\cos(\theta-\phi) \\ \quad -\sum_{m=2}^{\infty}\left[\frac{1}{m(m+1)}\frac{R^{m+2}}{\rho^m} - \frac{1}{m(m-1)}\frac{R^m}{\rho^{m-2}}\right]\cos[m(\theta-\phi)], \quad \rho > R \qquad (23b) \end{cases}$$

where the superscripts "I" and "E" denote the interior and exterior cases of $U(s,x)$ kernel depending on the geometry as shown in Fig. 2. The other kernels in the boundary integral equations can be obtained by utilizing the operators of Eqs. (12)–(14) with respect to the $U(s,x)$ kernel. The degenerate kernels U, Θ, M, V, U_θ, Θ_θ, M_θ, and V_θ in Eqs. (15) and (16) are listed in Appendix A. It is noted that the interior and exterior cases of U, Θ, M, U_θ, and Θ_θ are the same when they both approach to the boundary (ρ=R), since the degenerate kernels are continuous functions across the boundary. Then, the kernel function with the superscript "I"is chosen while the field point is inside the circular region; otherwise, the kernels with the superscript "E" are chosen.

4 Adaptive Observer System and Vector Decomposition for the Slope

4.1 Adaptive Observer System. Consider a plate problem with circular boundaries as shown in Fig. 3. Since the boundary integral equations are frame indifferent, i.e., rule of objectivity is obeyed. Adaptive observer system is chosen to fully employ the circular property by expanding the kernels into degenerate forms. The origin of the observer system can be adaptively located on the center of the corresponding boundary contour under integration. The dummy variable in the circular contour integration is the angle (θ) instead of radial coordinate (R). By using the adaptive

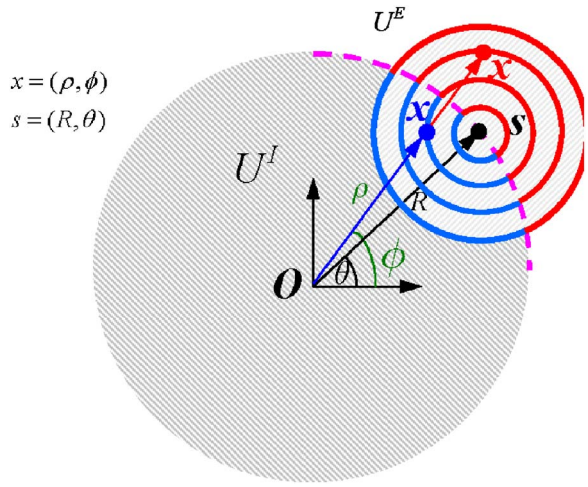

Fig. 2 Degenerate kernel for $U(s,x)$

system, all the boundary integrals can be determined analytically free of principal value senses.

4.2 Vector Decomposition. Since the higher-order singular equation is also one alternative to deal with the plate problem, potential gradient or higher-order gradients is required to calculate carefully. For the non-concentric case, special treatment for the potential gradient should be given as the source and field points locate on different circular boundaries. As shown in Fig. 4, the true normal direction with respect to the collocation point x on the B_i boundary can be superimposed by using the radial direction $\underset{\sim}{e}_\rho$ and angular direction $\underset{\sim}{e}_\phi$ on the B_j boundary. The degenerate kernels in Eq. (16) for the higher-order singular equation are changed to

$$U_n(s,x)=\frac{\partial U(s,x)}{\partial n_x}\cos(\phi-\phi')+\frac{\partial U(s,x)}{\partial t_x}\cos\left(\frac{\pi}{2}-\phi+\phi'\right) \tag{24}$$

$$\Theta_n(s,x)=\frac{\partial \Theta(s,x)}{\partial n_x}\cos(\phi-\phi')+\frac{\partial \Theta(s,x)}{\partial t_x}\cos\left(\frac{\pi}{2}-\phi+\phi'\right) \tag{25}$$

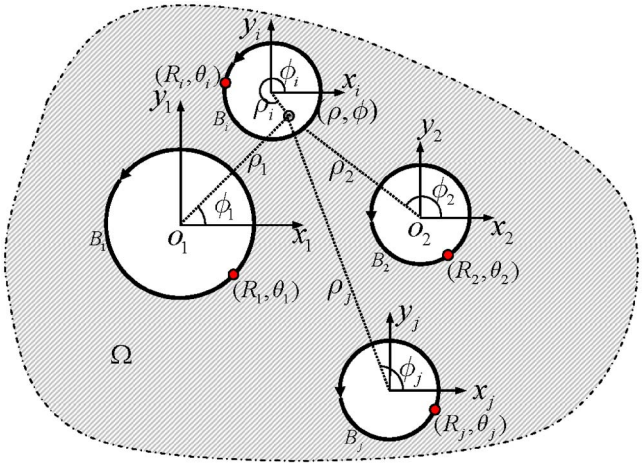

Fig. 3 Adaptive observer system when integrating the corresponding circular boundaries

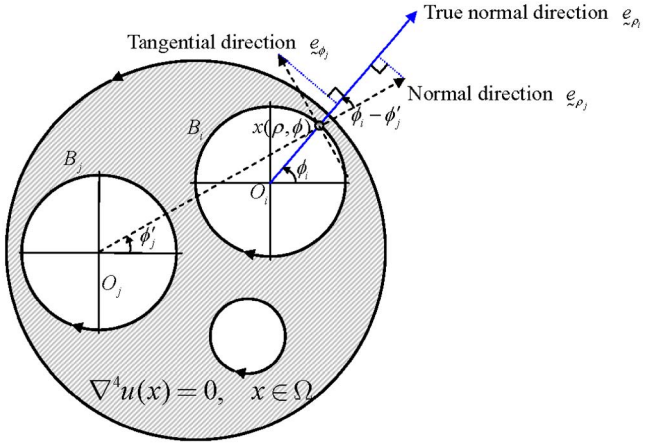

Fig. 4 Vector decomposition (collocation on x and integration on B_j)

$$M_n(s,x)=\frac{\partial M(s,x)}{\partial n_x}\cos(\phi-\phi')+\frac{\partial M(s,x)}{\partial t_x}\cos\left(\frac{\pi}{2}-\phi+\phi'\right) \tag{26}$$

$$V_n(s,x)=\frac{\partial V(s,x)}{\partial n_x}\cos(\phi-\phi')+\frac{\partial V(s,x)}{\partial t_x}\cos\left(\frac{\pi}{2}-\phi+\phi'\right) \tag{27}$$

The tangential derivative $\partial/\partial t_x$ with respect to the field point x for the four kernels needs to be additionally derived and is listed in Appendix A, where the normal derivative $\partial/\partial n_x$ is $\partial/\partial\rho$, and has been derived in the U_θ, Θ_θ, M_θ, and V_θ kernels. We call this treatment "vector decomposition technique." By approaching the collocation point from Ω^C to B_i and integrating circle B_j using the adaptive observer system of origin O_j, the normal and tangent derivatives can be superimposed as follows

$$\frac{\partial}{\partial\rho_i}=\frac{\partial}{\partial\rho_j}\cos(\phi_i-\phi_j')+\frac{1}{\rho_j}\frac{\partial}{\partial\phi_j}\cos\left(\frac{\pi}{2}-\phi_i+\phi_j'\right) \tag{28}$$

$$\frac{1}{\rho_i}\frac{\partial}{\partial\phi_i}=\frac{\partial}{\partial\rho_j}\cos\left(\frac{\pi}{2}-\phi_i+\phi_j'\right)+\frac{1}{\rho_j}\frac{\partial}{\partial\phi_j}\cos(\phi_i-\phi_j') \tag{29}$$

5 Linear Algebraic System

Consider the plate problem with circular domain containing N_h randomly distributed circular holes centered at the position vector $\underset{\sim}{c}_j$ $(j=1,2,\ldots,N)$, $(N=N_h+1$ and $\underset{\sim}{c}_1$ is the position vector of the outer circular boundary for the plate), as shown in Fig. 5 in which R_j denotes the radius of the jth circular region and B_j is the boundary of the jth circular hole. By uniformly collocating the $2M+1$ points x on each circular boundary in Eqs. (15) and (16), we have

$$0=\sum_{j=1}^{N}\int_{B_j}\{-U(s,x)v(s)+\Theta(s,x)m(s)-M(s,x)\theta(s)+V(s,x)u(s)\}dB_j(s),\quad x\in\Omega^C \tag{30}$$

$$0=\sum_{j=1}^{N}\int_{B_j}\{-U_\theta(s,x)v(s)+\Theta_\theta(s,x)m(s)-M_\theta(s,x)\theta(s)+V_\theta(s,x)u(s)\}dB_j(s),\quad x\in\Omega^C \tag{31}$$

It is noted that we select the null-field point on the boundary in the real computation. The selection of interior or exterior degenerate kernels depends on $r<R$ or $r>R$, respectively, according to the

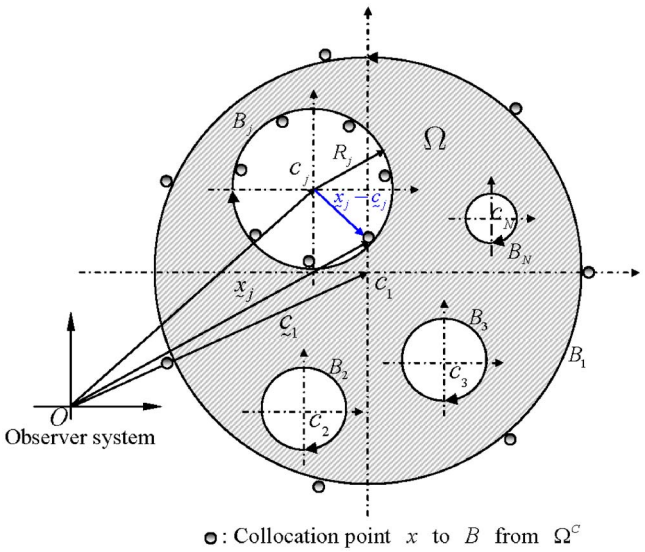

Fig. 5 Collocation point and boundary contour integration in the null-field integral equation

observer system. Besides, the path is counterclockwise for the outer circle; otherwise, it is clockwise. For the integral of the circular boundary, the degenerate kernels of $U(s,x)$, $\Theta(s,x)$, $M(s,x)$, $V(s,x)$, $U_\theta(s,x)$, $\Theta_\theta(s,x)$, $M_\theta(s,x)$, and $V_\theta(s,x)$ are utilized while the boundary densities of $u(s)$, $\theta(s)$, $m(s)$, and $v(s)$ along the circular boundary are substituted by using the Fourier series of Eqs. (19)–(22), respectively. In the B_j integration, the origin of the observer system is adaptively set to collocate at the center c_j to novelly utilize the degenerate kernels and Fourier series. A linear algebraic system

$$\begin{bmatrix} \mathbf{U}11 & \mathbf{\Theta}11 & \mathbf{U}12 & \mathbf{\Theta}12 & \cdots & \mathbf{U}1N & \mathbf{\Theta}1N \\ \mathbf{U}11_\theta & \mathbf{\Theta}11_\theta & \mathbf{U}12_\theta & \mathbf{\Theta}12_\theta & \cdots & \mathbf{U}1N_\theta & \mathbf{\Theta}1N_\theta \\ \mathbf{U}21 & \mathbf{\Theta}21 & \mathbf{U}22 & \mathbf{\Theta}22 & \cdots & \mathbf{U}2N & \mathbf{\Theta}2N \\ \mathbf{U}21_\theta & \mathbf{\Theta}21_\theta & \mathbf{U}22_\theta & \mathbf{\Theta}22_\theta & \cdots & \mathbf{U}2N_\theta & \mathbf{\Theta}2N_\theta \\ \vdots & \vdots & \vdots & \vdots & \ddots & \vdots & \vdots \\ \mathbf{U}N1 & \mathbf{\Theta}N1 & \mathbf{U}N2 & \mathbf{\Theta}N2 & \cdots & \mathbf{U}NN & \mathbf{\Theta}NN \\ \mathbf{U}N1_\theta & \mathbf{\Theta}N1_\theta & \mathbf{U}N2_\theta & \mathbf{\Theta}N2_\theta & \cdots & \mathbf{U}NN_\theta & \mathbf{\Theta}NN_\theta \end{bmatrix} \begin{Bmatrix} \mathbf{v}_1 \\ \mathbf{m}_1 \\ \mathbf{v}_2 \\ \mathbf{m}_2 \\ \vdots \\ \mathbf{v}_N \\ \mathbf{m}_N \end{Bmatrix}$$

$$= \begin{bmatrix} \mathbf{M}11 & \mathbf{V}11 & \mathbf{M}12 & \mathbf{V}12 & \cdots & \mathbf{M}1N & \mathbf{V}1N \\ \mathbf{M}11_\theta & \mathbf{V}11_\theta & \mathbf{M}12_\theta & \mathbf{V}12_\theta & \cdots & \mathbf{M}1N_\theta & \mathbf{V}1N_\theta \\ \mathbf{M}21 & \mathbf{V}21 & \mathbf{M}22 & \mathbf{V}22 & \cdots & \mathbf{M}2N & \mathbf{V}2N \\ \mathbf{M}21_\theta & \mathbf{V}21_\theta & \mathbf{M}22_\theta & \mathbf{V}22_\theta & \cdots & \mathbf{M}2N_\theta & \mathbf{V}2N_\theta \\ \vdots & \vdots & \vdots & \vdots & \ddots & \vdots & \vdots \\ \mathbf{M}N1 & \mathbf{V}N1 & \mathbf{M}N2 & \mathbf{V}N2 & \cdots & \mathbf{M}NN & \mathbf{V}NN \\ \mathbf{M}N1_\theta & \mathbf{V}N1_\theta & \mathbf{M}N2_\theta & \mathbf{V}N2_\theta & \cdots & \mathbf{M}NN_\theta & \mathbf{V}NN_\theta \end{bmatrix}$$

$$\times \begin{Bmatrix} \boldsymbol{\theta}_1 \\ \mathbf{u}_1 \\ \boldsymbol{\theta}_2 \\ \mathbf{u}_2 \\ \vdots \\ \boldsymbol{\theta}_N \\ \mathbf{u}_N \end{Bmatrix} \tag{32}$$

is obtained, where N denotes the number of circular boundaries (including inner and outer circular boundaries). For brevity, a unified form $[\mathbf{U}ij]$ ($i=1,2,3,\ldots,N$ and $j=1,2,3,\ldots,N$) denote the response of $U(s,x)$ kernel at the ith circle point due to the source at the jth circle. Otherwise, the same definition for $[\mathbf{\Theta}ij]$, $[\mathbf{M}ij]$, $[\mathbf{V}ij]$, $[\mathbf{U}ij_\theta]$, $[\mathbf{\Theta}ij_\theta]$, $[\mathbf{M}ij_\theta]$, and $[\mathbf{V}ij_\theta]$ cases. The submatrices of $[\mathbf{U}ij]$, $[\mathbf{\Theta}ij]$, $[\mathbf{M}ij]$, $[\mathbf{V}ij]$, $[\mathbf{U}ij_\theta]$, $[\mathbf{\Theta}ij_\theta]$, $[\mathbf{M}ij_\theta]$, and $[\mathbf{V}ij_\theta]$ are defined as follows

$$[\mathbf{U}ij] = \begin{bmatrix} Uij^{0c}(\phi_1) & Uij^{1c}(\phi_1) & Uij^{1s}(\phi_1) & \cdots & Uij^{Mc}(\phi_1) & Uij^{Ms}(\phi_1) \\ Uij^{0c}(\phi_2) & Uij^{1c}(\phi_2) & Uij^{1s}(\phi_2) & \cdots & Uij^{Mc}(\phi_2) & Uij^{Ms}(\phi_2) \\ Uij^{0c}(\phi_3) & Uij^{1c}(\phi_3) & Uij^{1s}(\phi_3) & \cdots & Uij^{Mc}(\phi_3) & Uij^{Ms}(\phi_3) \\ \vdots & \vdots & \vdots & \ddots & \vdots & \vdots \\ Uij^{0c}(\phi_{2M}) & Uij^{1c}(\phi_{2M}) & Uij^{1s}(\phi_{2M}) & \cdots & Uij^{Mc}(\phi_{2M}) & Uij^{Ms}(\phi_{2M}) \\ Uij^{0c}(\phi_{2M+1}) & Uij^{1c}(\phi_{2M+1}) & Uij^{1s}(\phi_{2M+1}) & \cdots & Uij^{Mc}(\phi_{2M+1}) & Uij^{Ms}(\phi_{2M+1}) \end{bmatrix} \tag{33}$$

$$[\mathbf{\Theta}ij] = \begin{bmatrix} \Theta ij^{0c}(\phi_1) & \Theta ij^{1c}(\phi_1) & \Theta ij^{1s}(\phi_1) & \cdots & \Theta ij^{Mc}(\phi_1) & \Theta ij^{Ms}(\phi_1) \\ \Theta ij^{0c}(\phi_2) & \Theta ij^{1c}(\phi_2) & \Theta ij^{1s}(\phi_2) & \cdots & \Theta ij^{Mc}(\phi_2) & \Theta ij^{Ms}(\phi_2) \\ \Theta ij^{0c}(\phi_3) & \Theta ij^{1c}(\phi_3) & \Theta ij^{1s}(\phi_3) & \cdots & \Theta ij^{Mc}(\phi_3) & \Theta ij^{Ms}(\phi_3) \\ \vdots & \vdots & \vdots & \ddots & \vdots & \vdots \\ \Theta ij^{0c}(\phi_{2M}) & \Theta ij^{1c}(\phi_{2M}) & \Theta ij^{1s}(\phi_{2M}) & \cdots & \Theta ij^{Mc}(\phi_{2M}) & \Theta ij^{Ms}(\phi_{2M}) \\ \Theta ij^{0c}(\phi_{2M+1}) & \Theta ij^{1c}(\phi_{2M+1}) & \Theta ij^{1s}(\phi_{2M+1}) & \cdots & \Theta ij^{Mc}(\phi_{2M+1}) & \Theta ij^{Ms}(\phi_{2M+1}) \end{bmatrix} \tag{34}$$

$$[\mathbf{M}ij] = \begin{bmatrix} Mij^{0c}(\phi_1) & Mij^{1c}(\phi_1) & Mij^{1s}(\phi_1) & \cdots & Mij^{Mc}(\phi_1) & Mij^{Ms}(\phi_1) \\ Mij^{0c}(\phi_2) & Mij^{1c}(\phi_2) & Mij^{1s}(\phi_2) & \cdots & Mij^{Mc}(\phi_2) & Mij^{Ms}(\phi_2) \\ Mij^{0c}(\phi_3) & Mij^{1c}(\phi_3) & Mij^{1s}(\phi_3) & \cdots & Mij^{Mc}(\phi_3) & Mij^{Ms}(\phi_3) \\ \vdots & \vdots & \vdots & \ddots & \vdots & \vdots \\ Mij^{0c}(\phi_{2M}) & Mij^{1c}(\phi_{2M}) & Mij^{1s}(\phi_{2M}) & \cdots & Mij^{Mc}(\phi_{2M}) & Mij^{Ms}(\phi_{2M}) \\ Mij^{0c}(\phi_{2M+1}) & Mij^{1c}(\phi_{2M+1}) & Mij^{1s}(\phi_{2M+1}) & \cdots & Mij^{Mc}(\phi_{2M+1}) & Mij^{Ms}(\phi_{2M+1}) \end{bmatrix} \tag{35}$$

$$[\mathbf{V}ij] = \begin{bmatrix} Vij^{0c}(\phi_1) & Vij^{1c}(\phi_1) & Vij^{1s}(\phi_1) & \cdots & Vij^{Mc}(\phi_1) & Vij^{Ms}(\phi_1) \\ Vij^{0c}(\phi_2) & Vij^{1c}(\phi_2) & Vij^{1s}(\phi_2) & \cdots & Vij^{Mc}(\phi_2) & Vij^{Ms}(\phi_2) \\ Vij^{0c}(\phi_3) & Vij^{1c}(\phi_3) & Vij^{1s}(\phi_3) & \cdots & Vij^{Mc}(\phi_3) & Vij^{Ms}(\phi_3) \\ \vdots & \vdots & \vdots & \ddots & \vdots & \vdots \\ Vij^{0c}(\phi_{2M}) & Vij^{1c}(\phi_{2M}) & Vij^{1s}(\phi_{2M}) & \cdots & Vij^{Mc}(\phi_{2M}) & Vij^{Ms}(\phi_{2M}) \\ Vij^{0c}(\phi_{2M+1}) & Vij^{1c}(\phi_{2M+1}) & Vij^{1s}(\phi_{2M+1}) & \cdots & Vij^{Mc}(\phi_{2M+1}) & Vij^{Ms}(\phi_{2M+1}) \end{bmatrix} \tag{36}$$

$$[\mathbf{U}ij_\theta] = \begin{bmatrix} Uij_\theta^{0c}(\phi_1) & Uij_\theta^{1c}(\phi_1) & Uij_\theta^{1s}(\phi_1) & \cdots & Uij_\theta^{Mc}(\phi_1) & Uij_\theta^{Ms}(\phi_1) \\ Uij_\theta^{0c}(\phi_2) & Uij_\theta^{1c}(\phi_2) & Uij_\theta^{1s}(\phi_2) & \cdots & Uij_\theta^{Mc}(\phi_2) & Uij_\theta^{Ms}(\phi_2) \\ Uij_\theta^{0c}(\phi_3) & Uij_\theta^{1c}(\phi_3) & Uij_\theta^{1s}(\phi_3) & \cdots & Uij_\theta^{Mc}(\phi_3) & Uij_\theta^{Ms}(\phi_3) \\ \vdots & \vdots & \vdots & \ddots & \vdots & \vdots \\ Uij_\theta^{0c}(\phi_{2M}) & Uij_\theta^{1c}(\phi_{2M}) & Uij_\theta^{1s}(\phi_{2M}) & \cdots & Uij_\theta^{Mc}(\phi_{2M}) & Uij_\theta^{Ms}(\phi_{2M}) \\ Uij_\theta^{0c}(\phi_{2M+1}) & Uij_\theta^{1c}(\phi_{2M+1}) & Uij_\theta^{1s}(\phi_{2M+1}) & \cdots & Uij_\theta^{Mc}(\phi_{2M+1}) & Uij_\theta^{Ms}(\phi_{2M+1}) \end{bmatrix} \tag{37}$$

$$[\mathbf{\Theta}ij_\theta] = \begin{bmatrix} \Theta ij_\theta^{0c}(\phi_1) & \Theta ij_\theta^{1c}(\phi_1) & \Theta ij_\theta^{1s}(\phi_1) & \cdots & \Theta ij_\theta^{Mc}(\phi_1) & \Theta ij_\theta^{Ms}(\phi_1) \\ \Theta ij_\theta^{0c}(\phi_2) & \Theta ij_\theta^{1c}(\phi_2) & \Theta ij_\theta^{1s}(\phi_2) & \cdots & \Theta ij_\theta^{Mc}(\phi_2) & \Theta ij_\theta^{Ms}(\phi_2) \\ \Theta ij_\theta^{0c}(\phi_3) & \Theta ij_\theta^{1c}(\phi_3) & \Theta ij_\theta^{1s}(\phi_3) & \cdots & \Theta ij_\theta^{Mc}(\phi_3) & \Theta ij_\theta^{Ms}(\phi_3) \\ \vdots & \vdots & \vdots & \ddots & \vdots & \vdots \\ \Theta ij_\theta^{0c}(\phi_{2M}) & \Theta ij_\theta^{1c}(\phi_{2M}) & \Theta ij_\theta^{1s}(\phi_{2M}) & \cdots & \Theta ij_\theta^{Mc}(\phi_{2M}) & \Theta ij_\theta^{Ms}(\phi_{2M}) \\ \Theta ij_\theta^{0c}(\phi_{2M+1}) & \Theta ij_\theta^{1c}(\phi_{2M+1}) & \Theta ij_\theta^{1s}(\phi_{2M+1}) & \cdots & \Theta ij_\theta^{Mc}(\phi_{2M+1}) & \Theta ij_\theta^{Ms}(\phi_{2M+1}) \end{bmatrix} \tag{38}$$

$$[\mathbf{M}ij_\theta] = \begin{bmatrix} Mij_\theta^{0c}(\phi_1) & Mij_\theta^{1c}(\phi_1) & Mij_\theta^{1s}(\phi_1) & \cdots & Mij_\theta^{Mc}(\phi_1) & Mij_\theta^{Ms}(\phi_1) \\ Mij_\theta^{0c}(\phi_2) & Mij_\theta^{1c}(\phi_2) & Mij_\theta^{1s}(\phi_2) & \cdots & Mij_\theta^{Mc}(\phi_2) & Mij_\theta^{Ms}(\phi_2) \\ Mij_\theta^{0c}(\phi_3) & Mij_\theta^{1c}(\phi_3) & Mij_\theta^{1s}(\phi_3) & \cdots & Mij_\theta^{Mc}(\phi_3) & Mij_\theta^{Ms}(\phi_3) \\ \vdots & \vdots & \vdots & \ddots & \vdots & \vdots \\ Mij_\theta^{0c}(\phi_{2M}) & Mij_\theta^{1c}(\phi_{2M}) & Mij_\theta^{1s}(\phi_{2M}) & \cdots & Mij_\theta^{Mc}(\phi_{2M}) & Mij_\theta^{Ms}(\phi_{2M}) \\ Mij_\theta^{0c}(\phi_{2M+1}) & Mij_\theta^{1c}(\phi_{2M+1}) & Mij_\theta^{1s}(\phi_{2M+1}) & \cdots & Mij_\theta^{Mc}(\phi_{2M+1}) & Mij_\theta^{Ms}(\phi_{2M+1}) \end{bmatrix} \tag{39}$$

$$[\mathbf{V}ij_\theta] = \begin{bmatrix} Vij_\theta^{0c}(\phi_1) & Vij_\theta^{1c}(\phi_1) & Vij_\theta^{1s}(\phi_1) & \cdots & Vij_\theta^{Mc}(\phi_1) & Vij_\theta^{Ms}(\phi_1) \\ Vij_\theta^{0c}(\phi_2) & Vij_\theta^{1c}(\phi_2) & Vij_\theta^{1s}(\phi_2) & \cdots & Vij_\theta^{Mc}(\phi_2) & Vij_\theta^{Ms}(\phi_2) \\ Vij_\theta^{0c}(\phi_3) & Vij_\theta^{1c}(\phi_3) & Vij_\theta^{1s}(\phi_3) & \cdots & Vij_\theta^{Mc}(\phi_3) & Vij_\theta^{Ms}(\phi_3) \\ \vdots & \vdots & \vdots & \ddots & \vdots & \vdots \\ Vij_\theta^{0c}(\phi_{2M}) & Vij_\theta^{1c}(\phi_{2M}) & Vij_\theta^{1s}(\phi_{2M}) & \cdots & Vij_\theta^{Mc}(\phi_{2M}) & Vij_\theta^{Ms}(\phi_{2M}) \\ Vij_\theta^{0c}(\phi_{2M+1}) & Vij_\theta^{1c}(\phi_{2M+1}) & Vij_\theta^{1s}(\phi_{2M+1}) & \cdots & Vij_\theta^{Mc}(\phi_{2M+1}) & Vij_\theta^{Ms}(\phi_{2M+1}) \end{bmatrix} \tag{40}$$

where ϕ_k ($k=1,2,3,\ldots,2M+1$) is the kth collocation angle of the collocation points on each boundary and the element of the submatrices are defined as follows

$$Uij^{nc}(\phi_k) = \int_{B_j} U(s,x_k)\cos(n\theta_j)dB_j(s), \quad n=0,1,2,3,\ldots,M \tag{41}$$

$$Uij^{ns}(\phi_k) = \int_{B_j} U(s,x_k)\sin(n\theta_j)dB_j(s), \quad n=1,2,3,\ldots,M \tag{42}$$

$$\Theta ij^{nc}(\phi_k) = \int_{B_j} \Theta(s,x_k)\cos(n\theta_j)dB_j(s), \quad n=0,1,2,3,\ldots,M \tag{43}$$

$$\Theta ij^{ns}(\phi_k) = \int_{B_j} \Theta(s,x_k)\sin(n\theta_j)dB_j(s), \quad n=1,2,3,\ldots,M \tag{44}$$

$$Mij^{nc}(\phi_k) = \int_{B_j} M(s,x_k)\cos(n\theta_j)dB_j(s), \quad n=0,1,2,3,\ldots,M \tag{45}$$

$$Mij^{ns}(\phi_k) = \int_{B_j} M(s,x_k)\sin(n\theta_j)dB_j(s), \quad n=1,2,3,\ldots,M \tag{46}$$

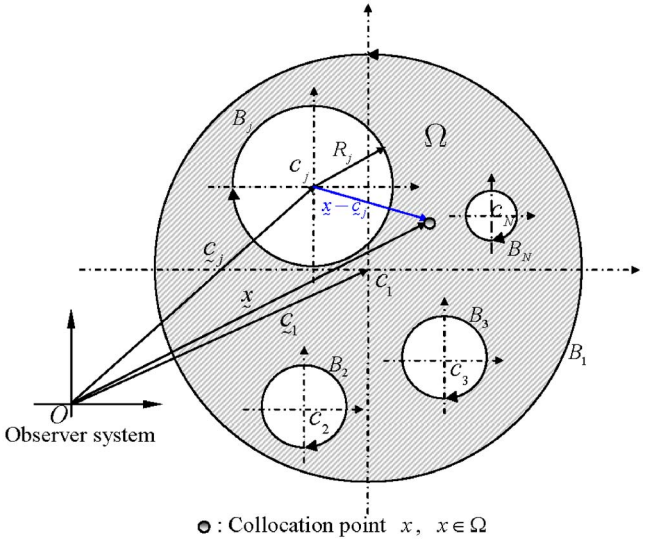

Fig. 6 Boundary integral equation for the domain point

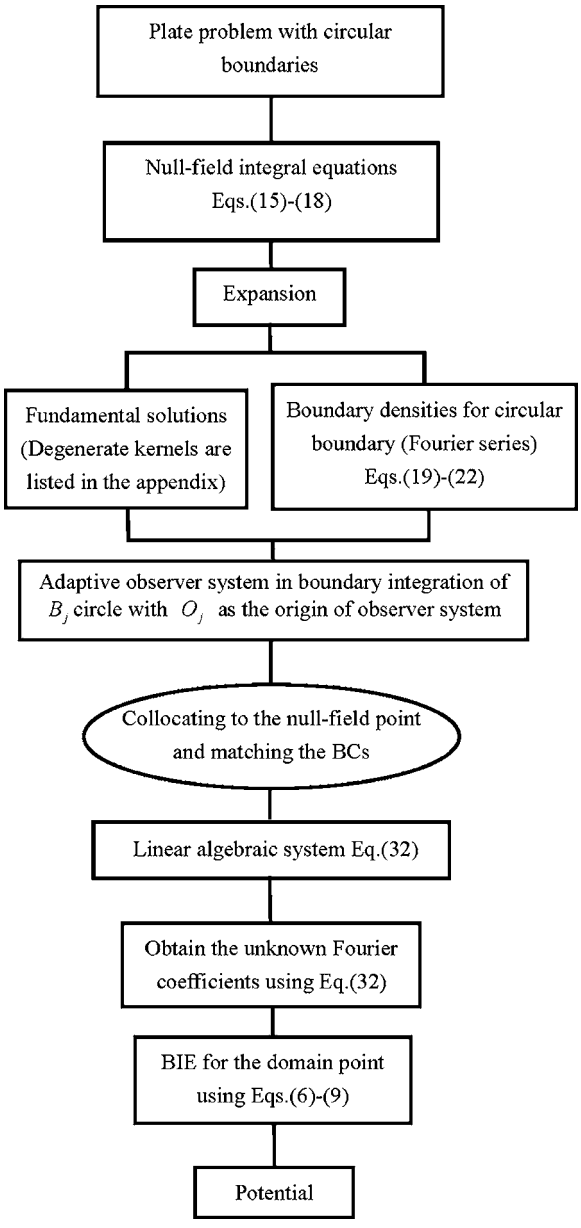

Fig. 7 Flowchart of the present method

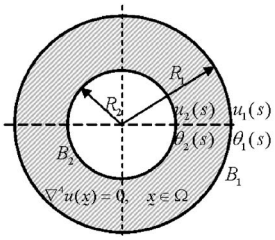

Geometric data:

$R_1 = 2$, $R_2 = 1$

Essential boundary conditions:

$u_1(s) = 0$ and $\theta_1(s) = 2\sin\theta$ on B_1

$u_2(s) = -3\sin\theta$ and $\theta_2(s) = 5\sin\theta$ on B_2

Fig. 8 An annular plate subject to the essential boundary conditions

$$Vij^{nc}(\phi_k) = \int_{B_j} V(s,x_k)\cos(n\theta_j)dB_j(s), \quad n = 0,1,2,3,\ldots,M \tag{47}$$

$$Vij^{ns}(\phi_k) = \int_{B_j} V(s,x_k)\sin(n\theta_j)dB_j(s), \quad n = 1,2,3,\ldots,M \tag{48}$$

$$Uij_{\theta}^{nc}(\phi_k) = \int_{B_j} U_{\theta}(s,x_k)\cos(n\theta_j)dB_j(s), \quad n = 0,1,2,3,\ldots,M \tag{49}$$

$$Uij_{\theta}^{ns}(\phi_k) = \int_{B_j} U_{\theta}(s,x_k)\sin(n\theta_j)dB_j(s), \quad n = 1,2,3,\ldots,M \tag{50}$$

$$\Theta ij_{\theta}^{nc}(\phi_k) = \int_{B_j} \Theta_{\theta}(s,x_k)\cos(n\theta_j)dB_j(s), \quad n = 0,1,2,3,\ldots,M \tag{51}$$

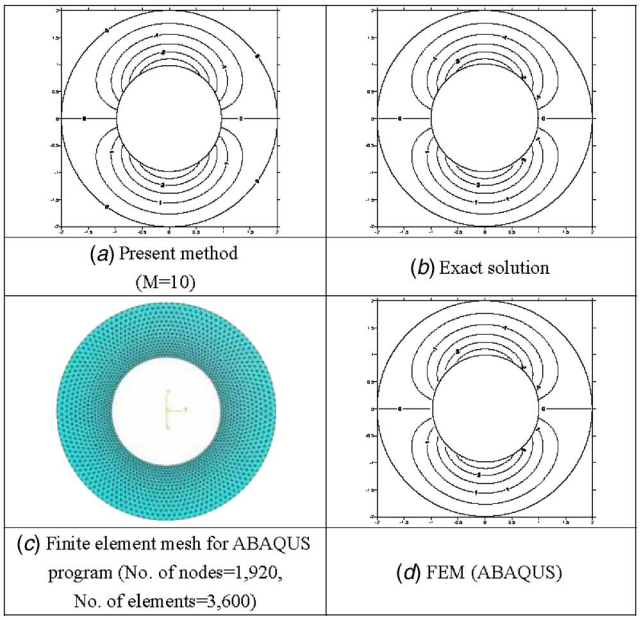

Fig. 9 The contour plot of displacement for the annular plate subject to the essential boundary conditions by using a different method

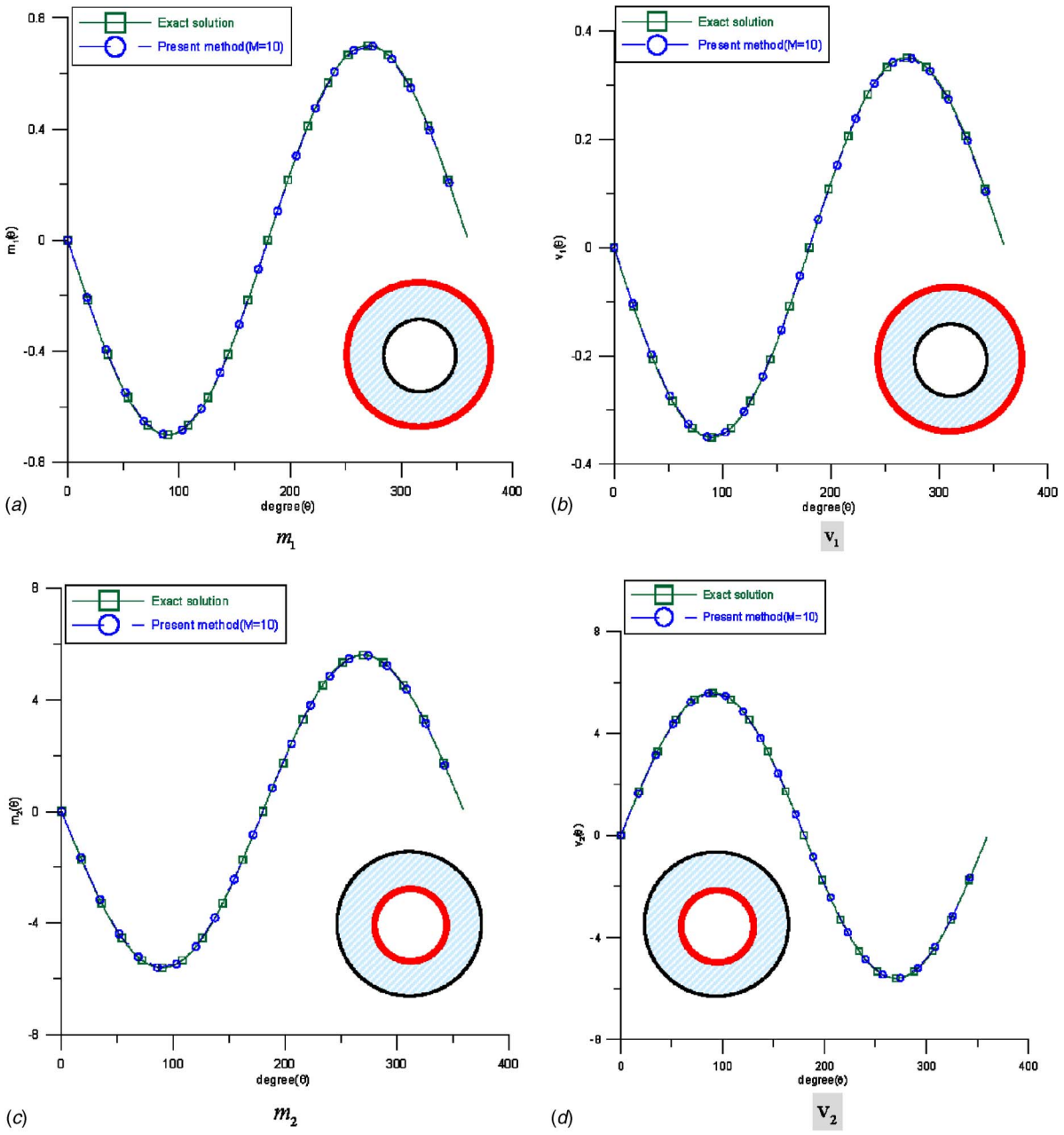

Fig. 10 Error estimation of the moment and shear force on the boundaries for the concentric circular domain

$$\Theta ij_{\theta}^{ns}(\phi_k) = \int_{B_j} \Theta_{\theta}(s,x_k)\sin(n\theta_j)dB_j(s), \quad n = 1,2,3,\ldots,M \tag{52}$$

$$Mij_{\theta}^{nc}(\phi_k) = \int_{B_j} M_{\theta}(s,x_k)\cos(n\theta_j)dB_j(s), \quad n = 0,1,2,3,\ldots,M \tag{53}$$

$$Mij_{\theta}^{ns}(\phi_k) = \int_{B_j} M_{\theta}(s,x_k)\sin(n\theta_j)dB_j(s), \quad n = 1,2,3,\ldots,M \tag{54}$$

$$Vij_{\theta}^{nc}(\phi_k) = \int_{B_j} V_{\theta}(s,x_k)\cos(n\theta_j)dB_j(s), \quad n = 0,1,2,3,\ldots,M \tag{55}$$

$$Vij_{\theta}^{ns}(\phi_k) = \int_{B_j} V_{\theta}(s,x_k)\sin(n\theta_j)dB_j(s), \quad n = 1,2,3,\ldots,M \tag{56}$$

where the interior degenerate kernels are used for $j=1$, $i=2,3,\ldots,N$ and $i=j=2,3,4,\ldots,N$; otherwise, exterior degenerate kernels are used. The explicit forms of the boundary integral for U kernel are listed in Appendix B. Finite value of singularity is obtained after introducing the degenerate kernel. Besides, the limiting case across the boundary ($R^-=r=R^+$) is also addressed. In-

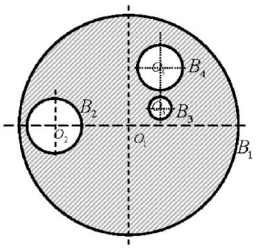

Geometric data:

$O_1=(0,0), R_1=20$; $O_2=(-14,0)$, $R_2=5$;
$O_3=(5,3)$, $R_3=2$; $O_4=(5,10)$, $R_4=4$

Essential boundary conditions:

$u(s)=0$ and $\theta(s)=0$ on B_1
$u(s)=\sin\theta$ and $\theta(s)=0$ on B_2
$u(s)=-1$ and $\theta(s)=0$ on B_3
$u(s)=1$ and $\theta(s)=0$ on B_4

Fig. 11 A circular plate containing three circular holes subject to the essential boundary conditions

stead of boundary data in BEM, the Fourier coefficients become the new unknown degree of freedom in the formulation. By rearranging the known and unknown sets, the Fourier coefficients can be obtained. Since the boundary data are determined, the displacement, slope, normal moment, and effective shear force of the plate can be solved by using the boundary integral equations for the domain point as shown in Fig. 6. The procedure of solution is described in a flowchart as shown in Fig. 7.

6 Numerical Results and Discussions

Case 1: An annular plate. An annular circular plate subject to the essential boundary conditions is considered as shown in Fig. 8. The unknown boundary densities of the plate are expressed in terms of Fourier series and the numerical result using fewer bases of Fourier series terms ($M=10$) is shown in Fig. 9(*a*). The annular case was also solved by using the FEM software (ABAQUS) [15] with 3,600 triangle elements as shown in Fig. 9(*c*). Good agreement is made after comparison with the exact solution,

$$u(\rho,\phi)=\rho\sin\phi-\frac{4}{\rho}\sin\phi,\quad 1<\rho<2,\quad 0\leq\phi<2\pi \tag{57}$$

as shown in Fig. 9(*b*) and the FEM result is shown in Fig. 9(*d*).

Since the exact solution is known, error estimation can be established. The boundary densities of the annular circular plate, normal moment, and effective shear force can be obtained by using the operators of Eqs. (13) and (14) with respect to the field point x. By substituting $\rho_1=2$ and $\rho_2=1$ into the two equations, the moment and the shear force on the boundaries of the annular plate are

$$m_1(x)=(\nu-1)\sin\phi,\quad x\in B_1,\quad 0\leq\phi<2\pi \tag{58}$$

$$v_1(x)=\frac{\nu-1}{2}\sin\phi\quad ,x\in B_1,\quad 0\leq\phi<2\pi \tag{59}$$

$$m_2(x)=8(\nu-1)\sin\phi,\quad x\in B_2,\quad 0\leq\phi<2\pi \tag{60}$$

$$v_2(x)=8(1-\nu)\sin\phi,\quad x\in B_2,\quad 0\leq\phi<2\pi \tag{61}$$

The numerical results of the moment and the shear force expanded in fewer bases of Fourier series ($M=10$) agree well with Eqs. (58)–(61) and are shown in Fig. 10.

Case 2: A circular plate with three holes [5]. A circular plate with the three circular holes which had been solved by Bird and Steele [5] is revisited by using the present method. The geometric data and the essential boundary conditions are shown in Fig. 11. The contour plots of displacement by using different numbers of terms in the Fourier series ($M=10,20,30,40,50$) are shown in Figs. 12(*a*)–12(*e*). It also shows that convergence is good with increasing of the terms of Fourier series. The case was also solved by using the ABAQUS software with 6,606 triangle elements as shown in Fig. 12(*g*). Good agreement among the data of Bird and Steele [5] as shown in Fig. 12(*f*), ABAQUS software results as shown in Fig. 12(*h*), and present solutions is obtained. To discuss the convergence of Fourier series, Parseval sum

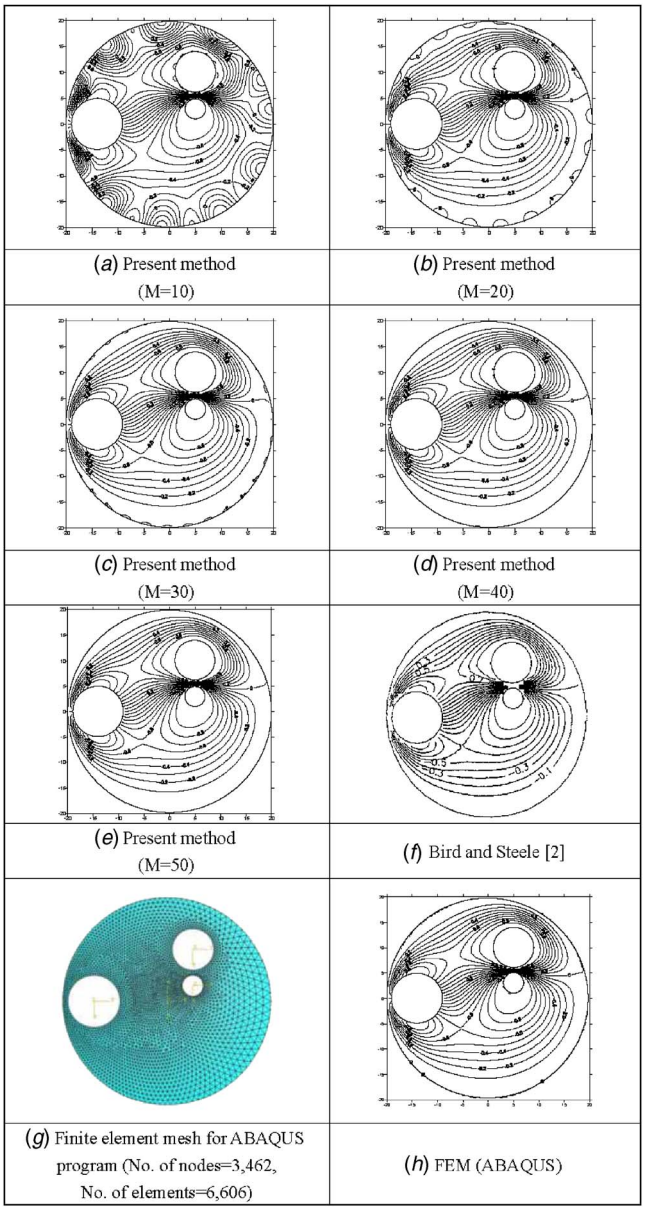

Fig. 12 The contour plots of displacement for the plate containing three circular holes subject to the essential boundary conditions by using different methods

$$\int_0^{2\pi} f^2(\theta)d\theta=2\pi a_0^2+\pi\sum_{n=1}^{\infty}(a_n^2+b_n^2) \tag{62}$$

versus terms of Fourier series with respect to m_1, v_1, m_2, v_2, m_3, v_3, m_4, v_4 (determined moment and shear force on the boundaries) are shown in Fig. 13, where $f(\theta)$ is the expansion of Fourier series and a_0, a_n, and b_n are the Fourier coefficients.

7 Conclusions

For plate problems with circular boundaries, a semi-analytical solution by using degenerate kernels, null-field integral equation, and Fourier series in an adaptive observer system was obtained. The main advantage of the present method over BEM is that all the improper integrals are transformed to series sum and can be

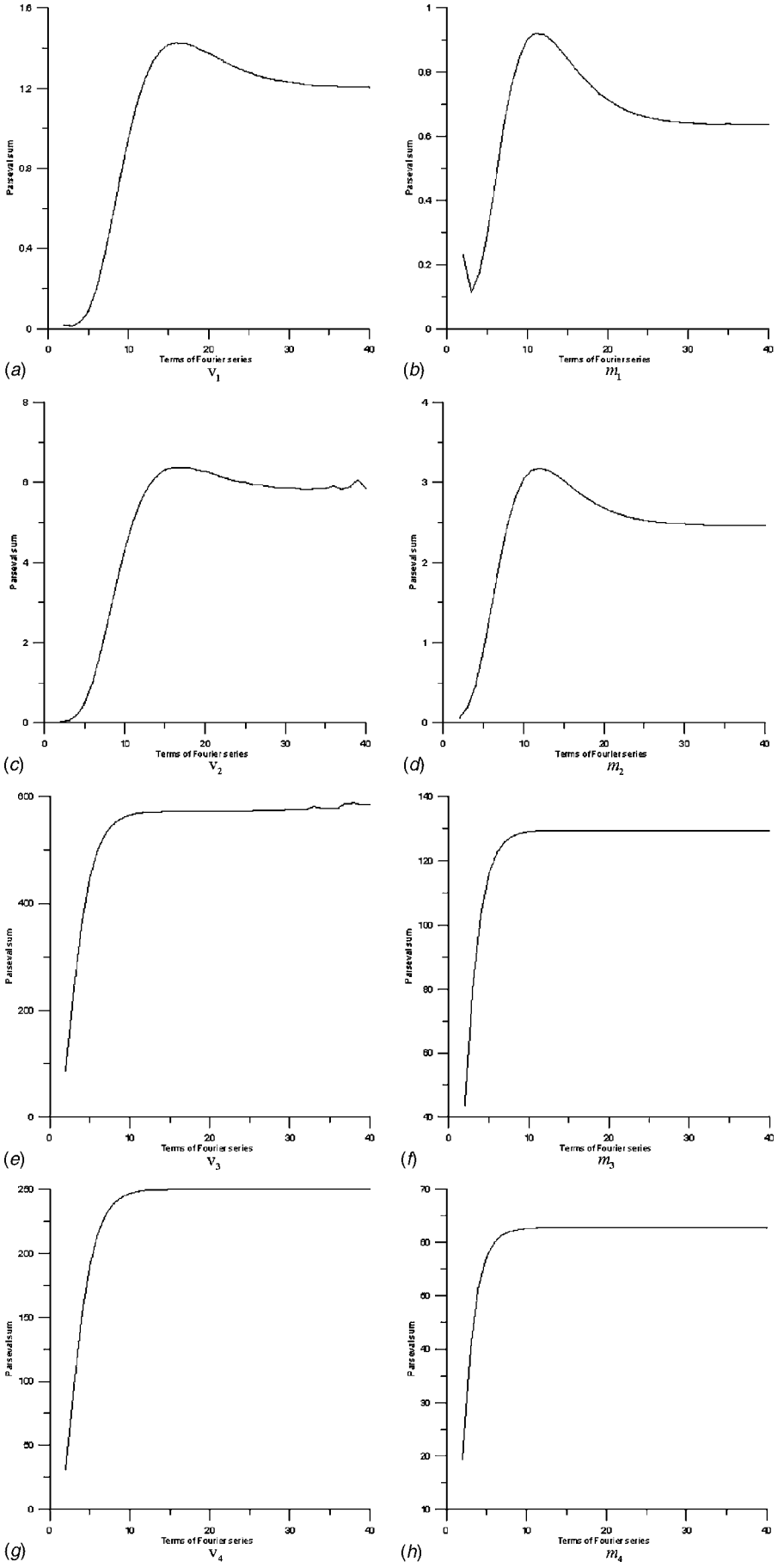

Fig. 13 Parseval sum versus terms of Fourier series

easily calculated when degenerate kernels are used. The potential across the boundary can be described explicitly from both sides (interior and exterior). Also, discretization of boundaries is not required. Once the Fourier coefficients of the unknown boundary densities were determined, the displacement, slope, moment, and shear force of the circular plate can be easily determined by substituting the boundary densities into the boundary integral equations for the domain point. Not only the annular plate but also the plate problems with multiple holes have been solved easily and effectively by using the present method in comparison with available exact solution and FEM results. The present method can be applied to plate containing arbitrary number of circular holes as well as various sizes and positions of circular holes. Finally, convergence study on the Fourier series was also done.

Appendix A: Degenerate Kernels

Degenerate kernels for U, Θ, M, V in the first boundary integral equation

$$
U(s,x)=\begin{cases}
U^I(s,x)=\rho^2(1+\ln R)+R^2\ln R-\left[R\rho(1+2\ln R)+\dfrac{1}{2}\dfrac{\rho^3}{R}\right]\cos(\theta-\phi)\\
\qquad -\displaystyle\sum_{m=2}^{\infty}\left[\frac{1}{m(m+1)}\frac{\rho^{m+2}}{R^m}-\frac{1}{m(m-1)}\frac{\rho^m}{R^{m-2}}\right]\cos[m(\theta-\phi)],\quad R\geqslant\rho\\
U^E(s,x)=R^2(1+\ln\rho)+\rho^2\ln\rho-\left[\rho R(1+2\ln\rho)+\dfrac{1}{2}\dfrac{R^3}{\rho}\right]\cos(\theta-\phi)\\
\qquad -\displaystyle\sum_{m=2}^{\infty}\left[\frac{1}{m(m+1)}\frac{R^{m+2}}{\rho^m}-\frac{1}{m(m-1)}\frac{R^m}{\rho^{m-2}}\right]\cos[m(\theta-\phi)],\quad \rho>R
\end{cases}
$$

$$
\Theta(s,x)=\begin{cases}
\Theta^I(s,x)=\dfrac{\rho^2}{R}+R(1+2\ln R)-\left[\rho(3+2\ln R)-\dfrac{1}{2}\dfrac{\rho^3}{R^2}\right]\cos(\theta-\phi)\\
\qquad +\displaystyle\sum_{m=2}^{\infty}\left[\frac{1}{m+1}\frac{\rho^{m+2}}{R^{m+1}}-\frac{m-2}{m(m-1)}\frac{\rho^m}{R^{m-1}}\right]\cos[m(\theta-\phi)],\quad R\geqslant\rho\\
\Theta^E(s,x)=2R(1+\ln\rho)-\left[\rho(1+2\ln\rho)+\dfrac{3}{2}\dfrac{R^2}{\rho}\right]\cos(\theta-\phi)\\
\qquad -\displaystyle\sum_{m=2}^{\infty}\left[\frac{m+2}{m(m+1)}\frac{R^{m+1}}{\rho^m}-\frac{1}{m-1}\frac{R^{m-1}}{\rho^{m-2}}\right]\cos[m(\theta-\phi)],\quad \rho>R
\end{cases}
$$

$$
M(s,x)=\begin{cases}
M^I(s,x)=(\nu-1)\dfrac{\rho^2}{R^2}+(\nu+3)+2(\nu+1)\ln R-\left[(\nu+1)-\dfrac{2\rho}{R}-(\nu-1)\dfrac{\rho^3}{R^3}\right]\cos(\theta-\phi)\\
\qquad +\displaystyle\sum_{m=2}^{\infty}\left[(\nu-1)\frac{\rho^{m+2}}{R^{m+2}}+\frac{m(1-\nu)-2(1+\nu)}{m}\frac{\rho^m}{R^m}\right]\cos[m(\theta-\phi)],\quad R\geqslant\rho\\
M^E(s,x)=2(1+\nu)(1+\ln\rho)-(\nu+3)\dfrac{R}{\rho}\cos(\theta-\phi)\\
\qquad +\displaystyle\sum_{m=2}^{\infty}\left[\frac{m(\nu-1)-2(\nu+1)}{m}\frac{R^m}{\rho^m}+(1-\nu)\frac{R^{m-2}}{\rho^{m-2}}\right]\cos[m(\theta-\phi)]\quad \rho>R
\end{cases}
$$

$$
V(s,x)=\begin{cases}
V^I(s,x)=\dfrac{4}{R}+\left[\dfrac{2\rho}{R^2}-(3-\nu)\dfrac{\rho^3}{R^4}(1-\nu)\right]\cos(\theta-\phi)\\
\qquad -\displaystyle\sum_{m=2}^{\infty}\left[m(1-\nu)\frac{\rho^{m+2}}{R^{m+3}}-(4+m(1-\nu))\frac{\rho^m}{R^{m+1}}\right]\cos[m(\theta-\phi)],\quad R>\rho\\
V^E(s,x)=(-3-\nu)\dfrac{1}{\rho}\cos(\theta-\phi)\\
\qquad +\displaystyle\sum_{m=2}^{\infty}\left[(m(1-\nu)-4)\frac{R^{m-1}}{\rho^m}-m(1-\nu)\frac{R^{m-3}}{\rho^{m-2}}\right]\cos[m(\theta-\phi)],\quad \rho>R
\end{cases}
$$

Degenerate kernels for U_θ, Θ_θ, M_θ, V_θ in the second boundary integral equation

$$U_\theta(s,x)=\begin{cases} U^I_\theta(s,x)=2\rho(1+\ln R)-\left[R(1+2\ln R)+\dfrac{3}{2}\dfrac{\rho^2}{R}\right]\cos(\theta-\phi) \\ \qquad -\displaystyle\sum_{m=2}^{\infty}\left[\frac{m+2}{m(m+1)}\frac{\rho^{m+1}}{R^m}-\frac{1}{m-1}\frac{\rho^{m-1}}{R^{m-2}}\right]\cos[m(\theta-\phi)], \quad R\geqslant\rho \\ U^E_\theta(s,x)=\dfrac{R^2}{\rho}+\rho(1+2\ln\rho)-\left[R(3+2\ln\rho)-\dfrac{1}{2}\dfrac{R^3}{\rho^2}\right]\cos(\theta-\phi) \\ \qquad +\displaystyle\sum_{m=2}^{\infty}\left[\frac{1}{m+1}\frac{R^{m+2}}{\rho^{m+1}}-\frac{m-2}{m(m-1)}\frac{R^m}{\rho^{m-1}}\right]\cos[m(\theta-\phi)], \quad \rho>R \end{cases}$$

$$\Theta_\theta(s,x)=\begin{cases} \Theta^I_\theta(s,x)=\dfrac{2\rho}{R}-\left[(3+2\ln R)-\dfrac{3}{2}\dfrac{\rho^2}{R^2}\right]\cos(\theta-\phi) \\ \qquad +\displaystyle\sum_{m=2}^{\infty}\left[\frac{m+2}{m+1}\frac{\rho^{m+1}}{R^{m+1}}-\frac{m-2}{m-1}\frac{\rho^{m-1}}{R^{m-1}}\right]\cos[m(\theta-\phi)], \quad R\geqslant\rho \\ \Theta^E_\theta(s,x)=\dfrac{2R}{\rho}-\left[(3+2\ln\rho)-\dfrac{3}{2}\dfrac{R^2}{\rho^2}\right]\cos(\theta-\phi) \\ \qquad +\displaystyle\sum_{m=2}^{\infty}\left[\frac{m+2}{m+1}\frac{R^{m+1}}{\rho^{m+1}}-\frac{m-2}{m-1}\frac{R^{m-1}}{\rho^{m-1}}\right]\cos[m(\theta-\phi)], \quad \rho>R \end{cases}$$

$$M_\theta(s,x)=\begin{cases} M^I_\theta(s,x)=\dfrac{2\rho}{R^2}(\nu-1)-\left[\dfrac{2}{R}(\nu+1)-3(\nu-1)\dfrac{\rho^2}{R^3}\right]\cos(\theta-\phi) \\ \qquad +\displaystyle\sum_{m=2}^{\infty}\left[(m+2)(\nu-1)\frac{\rho^{m+1}}{R^{m+2}}+(m(1-\nu)-2(1+\nu))\frac{\rho^{m-1}}{R^m}\right]\cos[m(\theta-\phi)], \quad R>\rho \\ M^E_\theta(s,x)=\dfrac{2(1+\nu)}{\rho}+(\nu+3)\dfrac{R}{\rho^2}\cos(\theta-\phi) \\ \qquad -\displaystyle\sum_{m=2}^{\infty}\left[(m(\nu-1)-2(\nu+1))\frac{R^m}{\rho^{m+1}}+(m-2)(1-\nu)\frac{R^{m-2}}{\rho^{m-1}}\right]\cos[m(\theta-\phi)], \quad \rho>R \end{cases}$$

$$V_\theta(s,x)=\begin{cases} V^I_\theta(s,x)=\left[\dfrac{2}{R^2}(3-\nu)-3(1-\nu)\dfrac{\rho^2}{R^4}\right]\cos(\theta-\phi) \\ \qquad -\displaystyle\sum_{m=2}^{\infty}\left[m(m+2)(1-\nu)\frac{\rho^{m+1}}{R^{m+3}}-m(4+m(1-\nu))\frac{\rho^{m-1}}{R^{m+1}}\right]\cos[m(\theta-\phi)], \quad R>\rho \\ V^E_\theta(s,x)=(3+\nu)\dfrac{1}{\rho^2}\cos(\theta-\phi) \\ \qquad -\displaystyle\sum_{m=2}^{\infty}\left[m(m(1-\nu)-4)\frac{R^{m-1}}{\rho^{m+1}}-m(m-2)(1-\nu)\frac{R^{m-3}}{\rho^{m-1}}\right]\cos[m(\theta-\phi)], \quad \rho>R \end{cases}$$

where U_θ, Θ_θ, M_θ, V_θ are equal to $\partial U(s,x)/\partial n_x$, $\partial\Theta(s,x)/\partial n_x$, $\partial M(s,x)/\partial n_x$, and $\partial V(s,x)/\partial n_x$, respectively.

Tangential derivative with respect to the field point

$$U_{,t}(s,x)=\begin{cases} U^I_{,t}(s,x)=-\left[R(1+2\ln R)+\frac{1}{2}\frac{\rho^2}{R}\right]\sin(\theta-\phi)-\sum_{m=2}^{\infty}\left[\frac{1}{m+1}\frac{\rho^{m+1}}{R^m}-\frac{1}{m-1}\frac{\rho^{m-1}}{R^{m-2}}\right]\sin[m(\theta-\phi)], & R>\rho \\ U^E_{,t}(s,x)=-\left[R(1+2\ln \rho)+\frac{1}{2}\frac{R^3}{\rho^2}\right]\sin(\theta-\phi)-\sum_{m=2}^{\infty}\left[\frac{1}{m+1}\frac{R^{m+2}}{\rho^{m+1}}-\frac{1}{m-1}\frac{R^m}{\rho^{m-1}}\right]\sin[m(\theta-\phi)], & \rho>R \end{cases}$$

$$\Theta_{,t}(s,x)=\begin{cases} \Theta^I_{,t}(s,x)=-\left(3+2\ln R-\frac{1}{2}\frac{\rho^2}{R^2}\right)\sin(\theta-\phi)+\sum_{m=2}^{\infty}\left[\frac{m}{m+1}\frac{\rho^{m+1}}{R^{m+1}}-\frac{m-2}{m-1}\frac{\rho^{m-1}}{R^{m-1}}\right]\sin[m(\theta-\phi)], & R>\rho \\ \Theta^E_{,t}(s,x)=-\left(1+2\ln \rho+\frac{3}{2}\frac{R^2}{\rho^2}\right)\sin(\theta-\phi)-\sum_{m=2}^{\infty}\left[\frac{m+2}{m+1}\frac{R^{m+1}}{\rho^{m+1}}-\frac{m}{m-1}\frac{R^{m-1}}{\rho^{m-1}}\right]\sin[m(\theta-\phi)], & \rho>R \end{cases}$$

$$M_{,t}(s,x)=\begin{cases} M^I_{,t}(s,x)=-\left[\frac{2(\nu+1)}{R}-(\nu-1)\frac{\rho^2}{R^3}\right]\sin(\theta-\phi) \\ \qquad +\sum_{m=2}^{\infty}\left[m(\nu-1)\frac{\rho^{m+1}}{R^{m+2}}+(m(1-\nu)-2(1+\nu))\frac{\rho^{m-1}}{R^m}\right]\sin[m(\theta-\phi)], & R>\rho \\ M^E_{,t}(s,x)=-(\nu+3)\frac{R}{\rho^2}\sin(\theta-\phi) \\ \qquad +\sum_{m=2}^{\infty}\left[(m(\nu-1)-2(\nu+1))\frac{R^m}{\rho^{m+1}}+m(1-\nu)\frac{R^{m-2}}{\rho^{m-1}}\right]\sin[m(\theta-\phi)], & \rho>R \end{cases}$$

$$V_{,t}(s,x)=\begin{cases} V^I_{,t}(s,x)=\left[\frac{2(3-\nu)}{R^2}-\frac{\rho^2}{R^4}(1-\nu)\right]\sin(\theta-\phi)-\sum_{m=2}^{\infty}\left[m^2(1-\nu)\frac{\rho^{m+1}}{R^{m+3}}-m(4+m(1-\nu))\frac{\rho^{m-1}}{R^{m+1}}\right]\sin[m(\theta-\phi)], & R>\rho \\ V^E_{,t}(s,x)=(-3-\nu)\frac{1}{\rho^2}\sin(\theta-\phi)+\sum_{m=2}^{\infty}\left[m(m(1-\nu)-4)\frac{R^{m-1}}{\rho^{m+1}}-m^2(1-\nu)\frac{R^{m-3}}{\rho^{m-1}}\right]\sin[m(\theta-\phi)], & \rho>R \end{cases}$$

Appendix B: Analytical Evaluation of the Integral and its Limit for $U(s,x)$ Kernel

	$U(s,x)$ and $\int_B U(s,x)t(s)dB(s)$
Degenerate kernel	$U(s,x)=\begin{cases} U^I(s,x)=\rho^2(1+\ln R)+R^2\ln R-\left[R\rho(1+2\ln R)+\frac{1}{2}\frac{\rho^3}{R}\right]\cos(\theta-\phi)-\sum_{m=2}^{\infty}\left[\frac{1}{m(m+1)}\frac{\rho^{m+2}}{R^m}-\frac{1}{m(m-1)}\frac{\rho^m}{R^{m-2}}\right]\cos[m(\theta-\phi)], & R\geqslant\rho \\ U^E(s,x)=R^2(1+\ln \rho)+\rho^2\ln \rho-\left[\rho R(1+2\ln \rho)+\frac{1}{2}\frac{R^3}{\rho}\right]\cos(\theta-\phi)-\sum_{m=2}^{\infty}\left[\frac{1}{m(m+1)}\frac{R^{m+2}}{\rho^m}-\frac{1}{m(m-1)}\frac{R^m}{\rho^{m-2}}\right]\cos[m(\theta-\phi)], & \rho>R \end{cases}$

Orthogonal process	$R \geqslant \rho$	$\int_0^{2\pi} U^I \cos(n\theta) R d\theta = \begin{cases} 0, n = \{0 \\ -\pi\left[R^2 \rho(1 + 2\ln R) + \frac{1}{2}\rho^3\right]\cos\phi, n = 1 \\ -\pi\left[R^2 \rho(1 + 2\ln R) + \frac{1}{2}\rho^3\right]\cos\phi - \pi\left[\frac{1}{n(n+1)}\frac{\rho^{n+2}}{R^{n+1}} - \frac{1}{n(n-1)}\frac{\rho^n}{R^{n-1}}\right]\cos(n\phi), n \geqslant 3 \end{cases}$ $\int_0^{2\pi} U^I \sin(n\theta) R d\theta = \begin{cases} 0, n = 1 \\ -\pi\left[R^2\rho(1 + 2\ln R) + \frac{1}{2}\rho^3\right]\sin\phi, n = 1 \\ -\pi\left[R^2\rho(1 + 2\ln R) + \frac{1}{2}\rho^3\right]\sin\phi - \pi\left[\frac{1}{n(n+1)}\frac{\rho^{n+2}}{R^{n+1}} - \frac{1}{n(n-1)}\frac{\rho^n}{R^{n-1}}\right]\sin(n\phi), n \geqslant 2 \end{cases}$
	$R < \rho$	$\int_0^{2\pi} U^E \cos(n\theta) R d\theta = \begin{cases} 0, n = 1 \\ -\pi\left[\rho R^2(1 + 2\ln\rho) + \frac{1}{2}\frac{R^4}{\rho}\right]\cos\phi, n = 1 \\ -\pi\left[\rho R^2(1 + 2\ln\rho) + \frac{1}{2}\frac{R^4}{\rho}\right]\cos\phi - \pi\left[\frac{1}{n(n+1)}\frac{R^{n+3}}{\rho^n} - \frac{1}{n(n-1)}\frac{R^{n+1}}{\rho^{n-2}}\right]\cos(n\phi), n \geqslant 2 \end{cases}$
	$R < \rho$	$\int_0^{2\pi} U^E \sin(n\theta) R d\theta = \begin{cases} 0, n = 1 \\ -\pi\left[\rho R^2(1 + 2\ln\rho) + \frac{1}{2}\frac{R^4}{\rho}\right]\sin\phi, n = 1 \\ -\pi\left[\rho R^2(1 + 2\ln\rho) + \frac{1}{2}\frac{R^4}{\rho}\right]\sin\phi - \pi\left[\frac{1}{n(n+1)}\frac{R^{n+3}}{\rho^n} - \frac{1}{n(n-1)}\frac{R^{n+1}}{\rho^{n-2}}\right]\sin(n\phi), n \geqslant 2 \end{cases}$
Limiting behavior $R^- = \rho = R^+$		$\lim_{\rho \to R} \int_0^{2\pi} U^I \cos(n\theta) R d\theta = \begin{cases} 0, n = 0 \\ -\pi\left[R^3(1 + 2\ln R) + \frac{1}{2}R^3\right]\cos\phi, n = 1 \\ -\pi\left[R^3(1 + 2\ln R) + \frac{1}{2}R^3\right]\cos\phi - \pi\left[\frac{1}{n(n+1)}R - \frac{1}{n(n-1)}R\right]\cos(n\phi), n \geqslant 2 \end{cases}$ $\lim_{\rho \to R} \int_0^{2\pi} U^I \sin(n\theta) R d\theta = \begin{cases} 0, n = 1 \\ -\pi\left[R^3(1 + 2\ln R) + \frac{1}{2}R^3\right]\sin\phi, n = 1 \\ -\pi\left[R^3(1 + 2\ln R) + \frac{1}{2}R^3\right]\sin\phi - \pi\left[\frac{1}{n(n+1)}R - \frac{1}{n(n-1)}R\right]\sin(n\phi), n \geqslant 2 \end{cases}$ $\lim_{\rho \to R} \int_0^{2\pi} U^E \cos(n\theta) R d\theta = \begin{cases} 0, n = 1 \\ -\pi\left[R^3(1 + 2\ln R) + \frac{1}{2}R^3\right]\cos\phi, n = 1 \\ -\pi\left[R^3(1 + 2\ln R) + \frac{1}{2}R^3\right]\cos\phi - \pi\left[\frac{1}{n(n+1)}R^3 - \frac{1}{n(n-1)}R^3\right]\cos(n\phi), n \geqslant 2 \end{cases}$ $\lim_{\rho \to R} \int_0^{2\pi} U^E \sin(n\theta) R d\theta = \begin{cases} 0, n = 1 \\ -\pi\left[R^3(1 + 2\ln R) + \frac{1}{2}R^3\right]\sin\phi, n = 1 \\ -\pi\left[R^3(1 + 2\ln\rho) + \frac{1}{2}R^3\right]\sin\phi - \pi\left[\frac{1}{n(n+1)}R^3 - \frac{1}{n(n-1)}R^3\right]\sin(n\phi), n \geqslant 2 \end{cases}$ (Continuous for $R^- < \rho < R^+$)

References

[1] Tanaka, M., Sladek, V., and Sladek, J., 1994, "Regularization Technique Applied to Boundary Element Methods," Appl. Mech. Rev., **47**, pp. 457–499.

[2] Sladek, J., and Sladek, V., 1982, "Three-Dimensional Crack Analysis for Anisotropic Body," Appl. Math. Model., **6**, pp. 374–380.

[3] Chen, J. T., Wu, C. S., and Chen, K. H., 2005, "A Study of Free Terms for Plate Problems in the Dual Boundary Integral Equations," Eng. Anal. Boundary Elem., **29**, pp. 435–446.

[4] Chen, J. T., Wu, C. S., Chen, K. H., and Lee, Y. T., 2005, "Degenerate Scale for Plate Analysis Using the Boundary Integral Equation Method and Boundary Element Method," Comput. Mech. (to be published).

[5] Bird, M. D., and Steele, C. R., 1991, "Separated Solution Procedure for Bending of Circular Plates with Circular Holes," Appl. Mech. Rev., **44**, pp. 27–35.

[6] Crouch, S. L., and Mogilevskaya, S. G., 2003, "On the Use of Somigliana's Formula and Fourier Series for Elasticity Problems with Circular Boundaries," Int. J. Numer. Methods Eng., **58**, pp. 537–578.

[7] Gradshteyn, I. S., and Ryzhik, I. M., 1996, *Table of Integrals, Series, and Products*, 5th ed., Academic, New York.

[8] Mogilevskaya, S. G., and Crouch, S. L., 2001, "A Galerkin Boundary Integral Method for Multiple Circular Elastic Inclusions," Int. J. Numer. Methods Eng., **52**, pp. 1069–1106.

[9] Chen, J. T., Wu, C. S., Lee, Y. T., and Chen, K. H., 2005, "On the Equivalence of the Trefftz Method and Method of Fundamental Solutions for Laplace and Biharmonic Equations," Comput. Math. Appl. (to be published).

[10] Bird, M. D., and Steele, C. R., 1992, "A Solution Procedure for Laplace's Equation on Multiple Connected Circular Domains," ASME J. Appl. Mech., **59**, pp. 398–404.

[11] Chen, J. T., Shen, W. C., and Wu, A. C., 2005, "Null-Field Integral Equation for Stress Field Around Circular Holes Under Antiplane Shear," Eng. Anal. Boundary Elements (to be published).

[12] Jeffery, G. B., 1921, "Plane Stress and Plane Strain in Bipolar Coordinates," Philos. Trans. R. Soc. London, Ser. A, **221**, pp. 265–293.

[13] Ling, C. B., 1948, "On the Stresses in a Plate Containing Two Circular Holes," J. Appl. Phys., **19**, pp. 77–82.

[14] Hsiao, C. C., 2005, "A Semi-Analytical Approach for Stokes Flow and Plate Problems With Circular Boundaries," Master's thesis, Department of Harbor and River Engineering, National Taiwan Ocean University, Keelung, Taiwan.

[15] ABAQUS/CAE 6.5, 2004. Hibbitt, Karlsson and Sorensen, Inc., RI.